

Estimations of the *S*-wave velocity structures in Chia-Yi City, Taiwan, using the array records of microtremors

Huey-Chu Huang and Cheng-Feng Wu

Institute of Seismology, National Chung Cheng University, Ming-Hsiung, Chia-Yi, Taiwan, R.O.C.

(Received May 20, 2005; Revised June 23, 2006; Accepted June 26, 2006; Online published December 25, 2006)

Shear-wave velocities (V_S) have been widely used for the site characterization of earthquake ground motion. We report here our investigation of the *S*-wave velocity structures of Chia-Yi City, Taiwan using the array records of microtremors at seven sites. The dispersion curves at these sites were first calculated using the F-K method proposed by Capon (1969); the *S*-wave velocity structures in Chia-Yi City were then estimated by employing the surface wave inversion technique (Herrmann, 1991). At frequencies lower than about 1 Hz, the propagation directions are concentrated in the northwest and southwest quadrants. The generation of these may be attributed to the ocean waves of the Taiwan Strait. The harder site (CBA) has higher phase velocities, while the softer sites (CWB, SHP and YRU) have lower phase velocities, especially at frequencies between 1 and 5 Hz. The shallow velocity structures (0–1,500 m) can be roughly divided into four to five layers. The depth of the alluvium gradually increases from east to west and from north to south.

Key words: Shear-wave velocity, microtremor, F-K method, surface wave inversion technique.

1. Introduction

For both theoretical simulations and ground motion predictions, it is essential to obtain concrete evidence pertaining to underground structures, especially for sedimentary layers overlying bedrock. While information on shear-wave velocity (V_S) in soil and rock substrates has frequently been used in earthquake engineering (Kramer, 1996), V_S data have, for the most part, been obtained using borehole methods. However, the drilling cost is relatively high, and non-intrusive surface methods are much more attractive options for obtaining V_S information in terms of costs. The Rayleigh-wave inversion technique using the array records of microtremors has been recognized as one of the most useful exploration methods to obtain the *S*-wave velocity structures of sedimentary layers in urbanized areas (Horike, 1985; Matsushima and Okada, 1990). In this method, long-period microtremors are used to estimate deep *S*-wave velocity structures, while short-period microtremors (<1 s) are used to estimate shallow ones. Based on the results of earlier studies, the array method has been applied to estimate not only deep but also shallow structures (Kawase *et al.*, 1998; Kudo *et al.*, 2002; Satoh *et al.*, 2001a, b). Liu *et al.* (2000) compared the phase velocities from the array measurements of Rayleigh waves associated with microtremors with those calculated from borehole shear-wave velocity profiles at two California sites. This comparison demonstrated quite clearly that this non-intrusive surface method can indeed provide adequate V_S information for ground-motion estimations. Satoh *et al.* (2001a) estimated deep *S*-wave velocity structures above the seismological

bedrock (pre-Tertiary bedrock) using the array records of microtremors in and around the Sendai basin, Japan. In a subsequent study, Satoh *et al.* (2001b) also estimated the *S*-wave velocity structures in a near-fault region of the Taichung basin, Taiwan, using both the array and single-station records of microtremors.

Chia-Yi City is located on the Chia-Nan Plain, a predominantly alluvial structure chiefly composed of shale, sandstone and conglomerate (Ho, 1986). The shallow velocity structures, as determined by seismic explorations, have been investigated by Shih *et al.* (1993), Shih and Fang (1994) and Shih (1995). In addition, Chung and Yeh (1997) studied the shallow crustal structures based on the short-period (1–5 s) Rayleigh-wave dispersion data of the 15 December 1993 Tapu earthquake ($M_L=5.8$) in southwestern Taiwan. Using the short-period fundamental Rayleigh waves with periods of 1.1–5.5 s, Hwang *et al.* (2003) have since investigated lateral variations in shallow-depth shear-wave structures up to a depth of 8 km under southwestern Taiwan. In the Chia-Nan area, the *P*-wave velocities at depths of 0–350 m range from 100 m/s to 500 m/s but, unfortunately, it is difficult to determine the near-surface *S*-wave velocity structures.

The 22 October 1999 Chia-Yi earthquake ($M_L=6.4$) and its major aftershock ($M_L=6.0$) struck the southwestern part of Taiwan. These two strong earthquakes also caused some damage in the area which covers—from north to south—Yun-Lin, Chia-Yi and Tai-Nan Counties (hereafter referred to as the Yun-Chia-Nan area). Several other destructive earthquakes have also occurred in this area in the past, which lies on this alluvial structure, thereby clearly indicating the necessity of studying the particular site effects (Huang, 2002).

In the study reported here, we conduct the array measure-

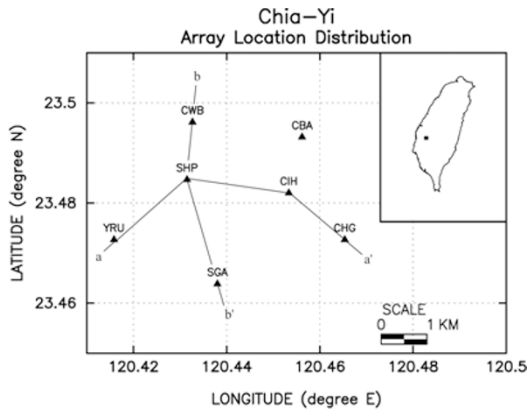


Fig. 1. Location map of the seven sites in Chia-Yi City at which the microtremor array measurements were carried out. Line a-a' represents the horizontal cross-section, line b-b' is the vertical cross-section.



Fig. 2. Three-dimensional view of the topography of Chia-Yi City. Gray scale bar indicates altitude.

ments of microtremors at seven sites in this area and also estimate the S-wave velocity structures beneath these sites.

2. Sites and Data

Located in the western part of Taiwan (Fig. 1), Chia-Yi City topographically extends across the Chia-Yi Hill and the Chia-Nan Plain (Fig. 2). The western and central parts of the city are on the alluvial plain, while the eastern part is on the hill. Two rivers, the Niuchouchi and the Pachangchi, flow through the northern and southern parts of Chia-Yi city, respectively (Fig. 2). Based on its topography, Chia-Yi city can be divided into two sections: (1) the eastern area, and (2) the western area.

Array measurements of microtremors were carried out using seven sets of portable instruments. Each set of instrument includes a tri-axial servo velocity sensor (VSE-315D), an amplifier, and a 24-bit digital recorder (SAMTAC-801B). This velocity sensor gives a flat amplitude from 0.1 to 70 Hz. The accuracy of the internal clock is within 1 ppm and is corrected by the Global Positioning System (GPS) before each measurement. The timing accuracy from GPS correction is within 1 ms. At each observation point, we continuously recorded microtremor measurements for about 68 min at a sampling frequency of 200 Hz.

Microtremor array measurements were carried out at

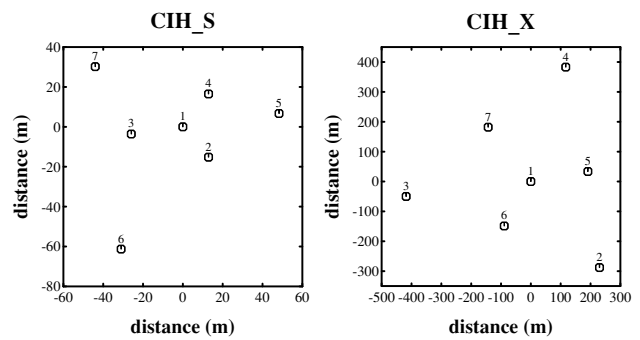


Fig. 3. Seven-element nested-triangular array configuration of the S-array and the X-array at the CIH site.

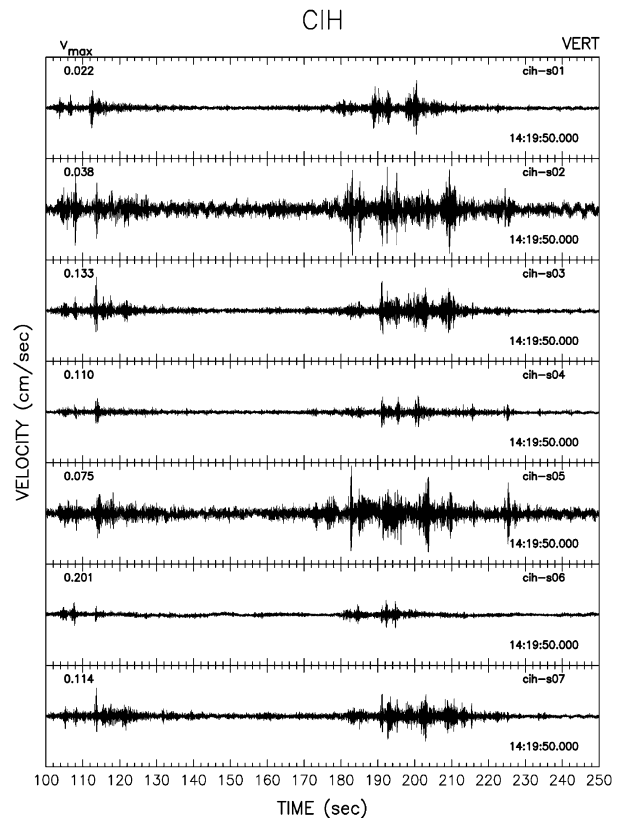


Fig. 4. Vertical microtremors recorded by the S array (s01-s07) at the CIH site.

seven sites (CBA, CHG, CIH, CWB, SGA, SHP and YRU), as shown in Figs. 1 and 2. We used seven observed points in each array deployment and four array measurements of different sizes (S, M, L and X) at each site. Figure 3 shows the array configurations in both the S and X size for site CIH, as an example. The central station (No. 1) is fixed for all of the arrays that are S (radius=50 m), M (radius=100 m), L (radius=200 m) and X (radius=400 m) arrays. The configuration of these seven stations is in the form of two different aperture triangles around the central station. The locations and array sizes, and maximum and minimum separations of instruments for the seven sites are tabulated in Table 1. The vertical component of the velocity waveforms of the S array at the CIH site is shown in Fig. 4. In general, the waveforms are similar to each other, especially at the

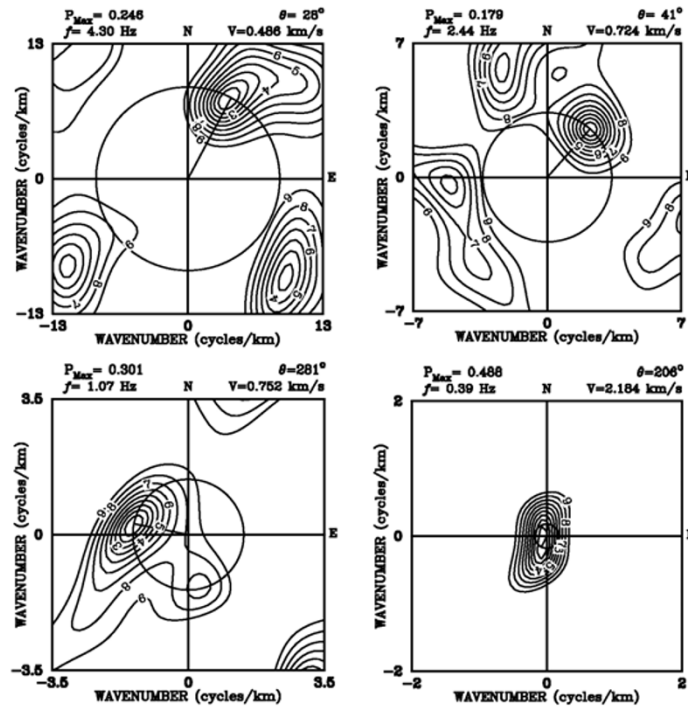


Fig. 5. f - k power spectra at 4.3, 2.44, 1.07 and 0.39 Hz calculated from the recordings observed from the S-, M-, L- and X- arrays, respectively, at the CIH site.

stations which are closest to each other (see Fig. 3 for the array configurations).

3. Methods of Analysis

3.1 F-K spectral analysis method

Two estimation methods have been used from more than three decades to analyze data from an array with non-uniform distances between neighboring sensors. This first is the frequency domain Beam-Forming Method (BFM) developed by Lacoss *et al.* (1969), while the second is the Maximum Likelihood Method (MLM) developed by Capon (1969). According to a number of researchers (Capon, 1969; Mack and Filnn, 1971; Woods and Lintz, 1973; Huang and Yeh, 1990), the resolving power of the MLM is higher than that of the BFM; however, these two methods do agree in the case of perfectly uncorrected array data.

The power spectrum at frequency f and vector wavenumber k for an array of N sensors following the MLM is given by:

$$P(f, k) = \left[\sum_{i,j=1}^N \phi_{ij}^{-1}(f) \exp(i\vec{k} \cdot \vec{r}_{ij}) \right]^{-1}, \quad (1)$$

where N is number of sensors; $\phi_{ij}(f)$ is cross-power spectrum between the i th and j th sensors at frequency f ; $\vec{r}_{ij} = \vec{r}_j - \vec{r}_i$ where \vec{r}_i and \vec{r}_j are the position vectors of the i th and j th sensors, respectively; $\phi_{ij}^{-1}(f)$ is the inverse of the coherence matrix $\phi_{ij}(f)$.

Based on the results of the f - k power spectrum, the phase velocity V can be estimated by:

$$V = f / \sqrt{k_{x_0}^2 + k_{y_0}^2}, \quad (2)$$

Table 1. Array locations, sizes, maximum and minimum separations between instruments for seven sites.

Site Name	Latitude (degree)	Longitude (degree)	Size	Min. Separation (m)	Max. Separation (m)
CBA	23.495	120.448	S	12.6	55.7
			M	24	171.8
			L	47.4	471.1
			X	183	718
CHG	23.474	120.457	S	28.4	94.8
			M	43	169.3
			L	84	493
CIH	23.484	120.446	S	20	104.5
			M	48.8	195.1
			L	96.1	365.7
CWB	23.498	120.425	X	177	691
			S	16.8	77.8
			M	34.6	173.8
			L	75.2	336.1
SGA	23.465	120.430	X	174	1064
			S	24.7	110.9
			M	49.4	170.3
			L	74.5	411.4
SHP	23.486	120.423	X	176	749
			S	20.6	99.2
			M	47.3	325.5
			L	114.2	422
YRU	23.474	120.408	X	169	752
			S	18.4	105
			M	56.7	248
			L	110.2	414.5
			X	208	800

where k_{x_0} and k_{y_0} correspond to the peak power positions in the wavenumber space.

3.2 Inversion of the velocity structure

The discrete generalized inversion method, devised by Wiggins (1972) and Jackson (1972), has previously been

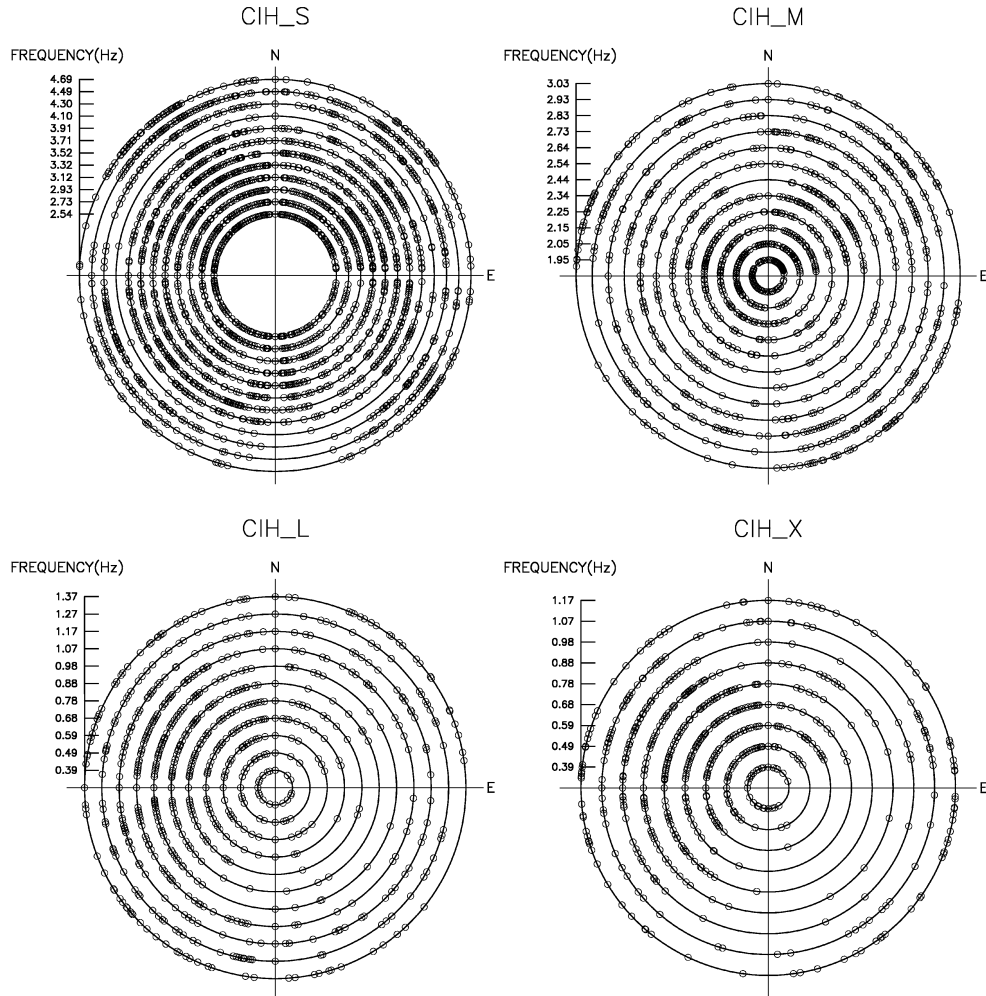


Fig. 6. Propagation directions as estimated from all of the f - k spectra for the four different arrays at the CIH site: (a) S-array; (b) M-array; (c) L-array; (d) X-array.

applied to determine S -wave velocity structures. The problem is written as:

$$Y = AX. \tag{3}$$

The vector Y of length n corresponds to the difference between the measured phase velocities and those calculated in the initial model. The vector X of length m , which is the solution we seek, corresponds to the first order correction for the initial model. Therefore, an inverted model is the sum of the initial model and the solution vector X . The generalized inversion method makes it possible to obtain the unique solution X even if the data Y are disturbed by random errors and n is not equal to m .

The relationship between the dispersion curve of surface-wave and the velocity structure is nonlinear. For convenience in structure inversion, a quasi-linear relationship between the dispersion curve and velocity structure will be retrieved through Taylor series expansion when the high-order terms are neglected. Because the phase velocities are more sensitive to the S -wave velocity structure than to the P -wave velocity and density structures (Horike, 1985), only the S -wave velocity is inverted in this study. The formula, which links the dispersion curve and velocity model param-

eters, can be written as follows (Hwang and Yu, 2005):

$$\Delta C(T_j) = \sum_{i=1}^N \left(\frac{\partial C(T_j)}{\partial \beta_i} \right) \Delta \beta_i \tag{4}$$

where $\Delta C(T_j)_i$ is the difference between the observed and predicted phase velocity derived from initial velocity model at the j th period (T_j); N is the number of layers; $\frac{\partial C(T_j)}{\partial \beta_i}$ is the partial derivative of the phase-velocity with respect to the S -wave velocity of the i th layer; $\Delta \beta_i$ is the resulting difference in the S -wave velocity of the i th layer between adjacent inversions.

Because the inversion of surface waves is inappropriate to resolve discontinuities in the Earth's interior, the velocity model is given as a velocity gradient. To solve model parameters ($\Delta \beta_i$) of Eq. (4), we employ a surface-wave inversion program based on damped least-squares (Herrmann, 1991). Smoothing constraints, the difference between adjacent model parameters as an approximation of a derivative to control solution roughness, were also used (see Menke, 1984). In this study, we construct a layered media overlying on the half-space medium as an initial model. The velocity is obtained by dividing the maximum phase velocity by 0.92 at the used lowest frequency (about 0.39 Hz). In

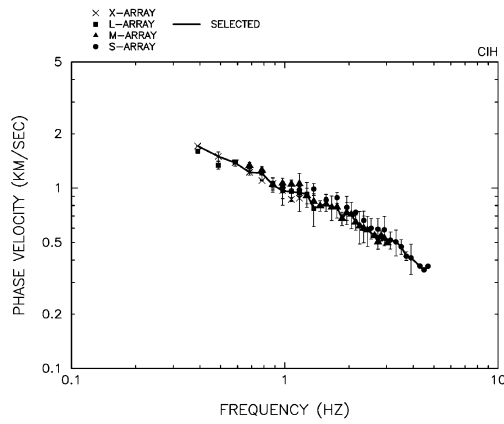


Fig. 7. Average and average ± 1 SD of the phase velocities obtained from the recordings at CIH. The different symbols represent the results from the different-sized arrays. The black line is the final phase velocity selected in this study.

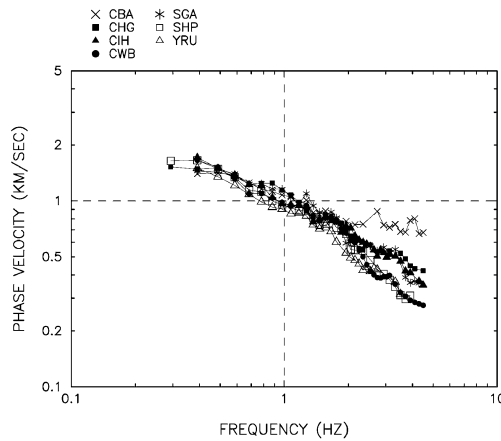


Fig. 8. Phase velocities obtained from the recordings observed at the seven different array sites. The estimated phase velocities vary from site to site.

addition, the total layer number and the thickness of each layer are designed to be 80 and 20 m. A damping value of 1.0 is adopted to stabilize the inversion. The inversion process will be terminated when the difference in S -wave velocity for each layer between the adjacent inversions is less than 0.001 km/s. Although the inversion of phase velocity is non-unique, we carefully evaluated the rationality of the inverted S -wave velocity and misfit between observed and theoretical phase velocities for each inversion. Hence, the reasonable velocity model would be obtained.

4. Results and Discussion

4.1 F-K analysis of the microtremor array data

By overlapping one-half of each window length, we divide the observed recordings of the vertical component into time segments with a length of 20.48 s for the S- and M-array recordings and 40.96 s for the L- and X-array recordings. After removing some segments that were clearly contaminated by instrumental noise and cultural sources, we estimate the phase velocities by performing the f - k spectral analysis based on the maximum likelihood method (Capon, 1969). Figure 5 shows the f - k spectra from the MLM using

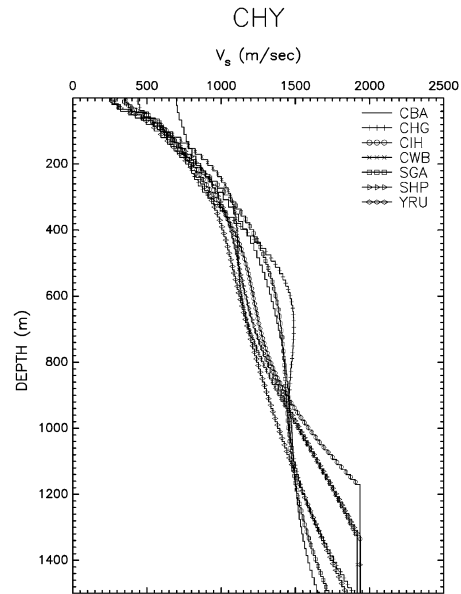


Fig. 9. Estimated S -wave velocity structures at the seven sites, as determined from the differential inversion technique (Herrmann, 1991). The different symbols represent the results for the different sites.

the microtremor data observed at the CIH site. We calculate the f - k spectra at 51×51 grid points at each frequency and at 4.3, 2.44, 1.07 and 0.39 Hz from the records on the S-, M-, L- and X- arrays, respectively. The propagation direction (θ) is measured clockwise from the north in degrees. We estimate the phase velocity (V) in km/s from the maximum peak in the f - k spectrum. Since we search the maximum peaks within the wavenumber windows that we set a priori, the minimum phase velocities are limited, but the maximum ones are not.

Figure 6 shows the propagation directions we estimate from all the selected f - k spectra for the S-, M-, L- and X-array at the CIH site. At frequencies lower than about 1 Hz, the propagation directions are concentrated in the northwest and southwest quadrants, which coincide with the direction of the coastal line of the Taiwan Strait. At higher frequencies, however, the propagation directions are relatively scattered.

According to Horike (1985), if the measured phase velocities are less than the S -wave velocity of the basement, which is believed to be higher than 2 km/s in most cases, and if they are normally dispersive, then it is reasonable to identify them as those of the surface waves. In all other cases, those signals must belong to the body waves. In addition, according to the shallow crustal structure in southwestern Taiwan (Chung and Yeh, 1997), S -wave velocity at the depth of 2.07 km is about 2.56 km/s. For these reasons, we exclude phase velocities higher than 3 km/s. Moreover, we also searched maximum (C_{max}) and minimum (C_{min}) phase velocities for each frequency and excluded unreliable phase velocities with a significance level of 10% of ($C_{max} - C_{min}$). We then chose a value by taking an average over the reliable phase velocities. The average and average ± 1 standard deviations of the phase velocities obtained from the recordings at CIH are shown in Fig. 7. The different symbols

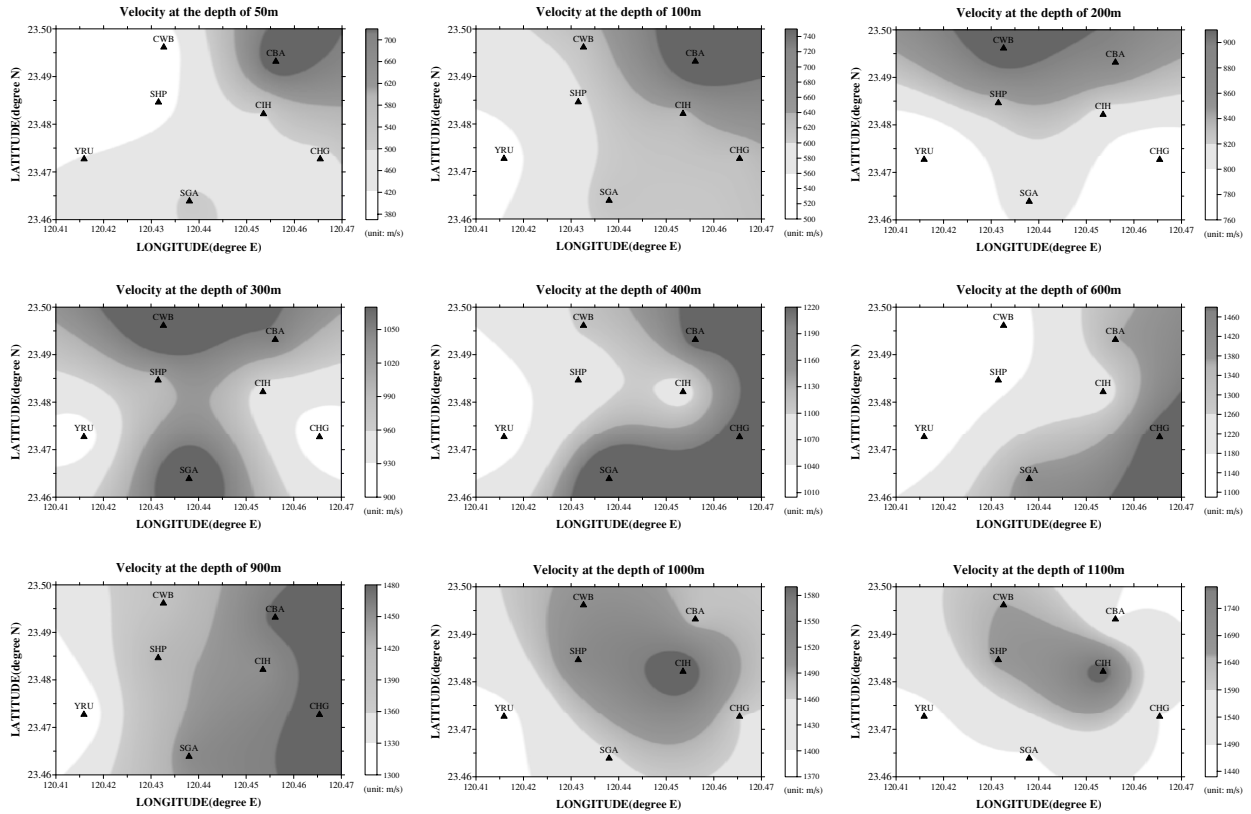


Fig. 10. S-wave velocity contours of Chia-Yi City at different depths between 50 m and 1,000 m based on the results shown in Fig. 9.

Table 2. Inverted S-wave velocity structures at the seven sites of Chia-Yi city.

Layer No.	YRU	SHP	CIH	CHG	CBA	CWB	SGA
1	312 (60)	265 (34)	361 (30)	330 (38)	-	247 (34)	327 (42)
2	584 (140)	693 (119)	624 (120)	589 (114)	698 (44)	464 (85)	558 (105)
3	971 (160)	914 (136)	971 (240)	865 (114)	998 (242)	908 (102)	968 (189)
4	1363 (360)	1329 (221)	1246 (375)	-	1378 (308)	1085 (374)	1271 (147)
5	1812 (620)	1704 (408)	1721 (195)	1517 (627)	1471 (682)	1165 (187)	1372 (168)
				1646 (323)	-		1439 (504)
							1537 (231)
							1733 (252)

Note: Number in parenthesis indicates thickness in meters.

represent the results from the different-sized arrays. The final phase velocities (the solid line in Fig. 7) are chosen by following the sequence of the X- ($0.3 \text{ Hz} \leq f < 0.7 \text{ Hz}$), L- ($0.7 \text{ Hz} \leq f < 1.1 \text{ Hz}$), M- ($1.1 \text{ Hz} \leq f < 3 \text{ Hz}$) and S- arrays ($3 \text{ Hz} \leq f \leq 5 \text{ Hz}$) from low frequencies to high frequencies. Basically, the results of the X- and L-arrays are stable at lower frequencies, whereas those of the S- and M- arrays are stable at higher frequencies.

Figure 8 presents the phase velocities that we obtain from the recordings of all the arrays. It is evident that the estimated phase velocities vary from site to site. Based on the shapes of the dispersion curves at the seven sites, we can divide these into three groups: (1) CBA; (2) CHG, CIH and SGA; (3) CWB, SHP and YRU. This grouping agrees well with their respective shallow geological conditions. The harder site, CBA, has higher phase velocities and is in sharp

contrast with the softer sites (CWB, SHP and YRU), which have lower phase velocities, especially at frequencies of 1–5 Hz.

4.2 Inversion of the S-wave velocity structures

We invert S-wave velocity structures using the method proposed by Herrmann (1991). The estimated S-wave velocity structures determined by the differential inversion technique at all seven sites are shown in Fig. 9. Compared with the other six sites, CBA has the highest S-wave velocities at depths of less than 140 m. If we assume that the S-wave velocity in the bedrock is 1,500 m/s, then the alluvial thickness of Chia-Yi City is about 1,000–1,200 m.

To understand the variations in the shallow S-wave velocities in Chia-Yi City, the S-wave velocity contours at depths of 50–1,100 m, based on the results in Fig. 9, are shown in Fig. 10. Some features of these results are summarized as

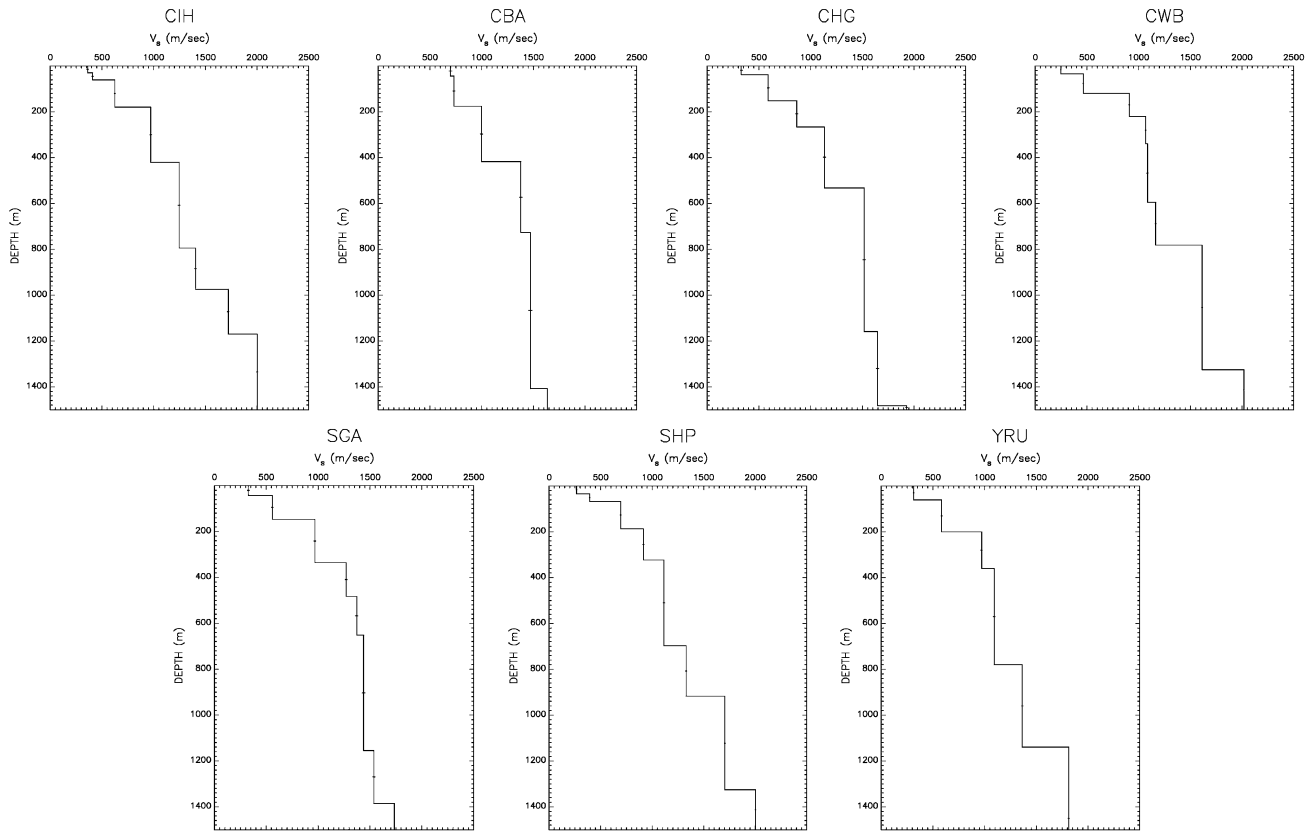


Fig. 11. Estimated *S*-wave velocity structures at the seven sites, as determined from the stochastic inversion technique (Herrmann, 1991).

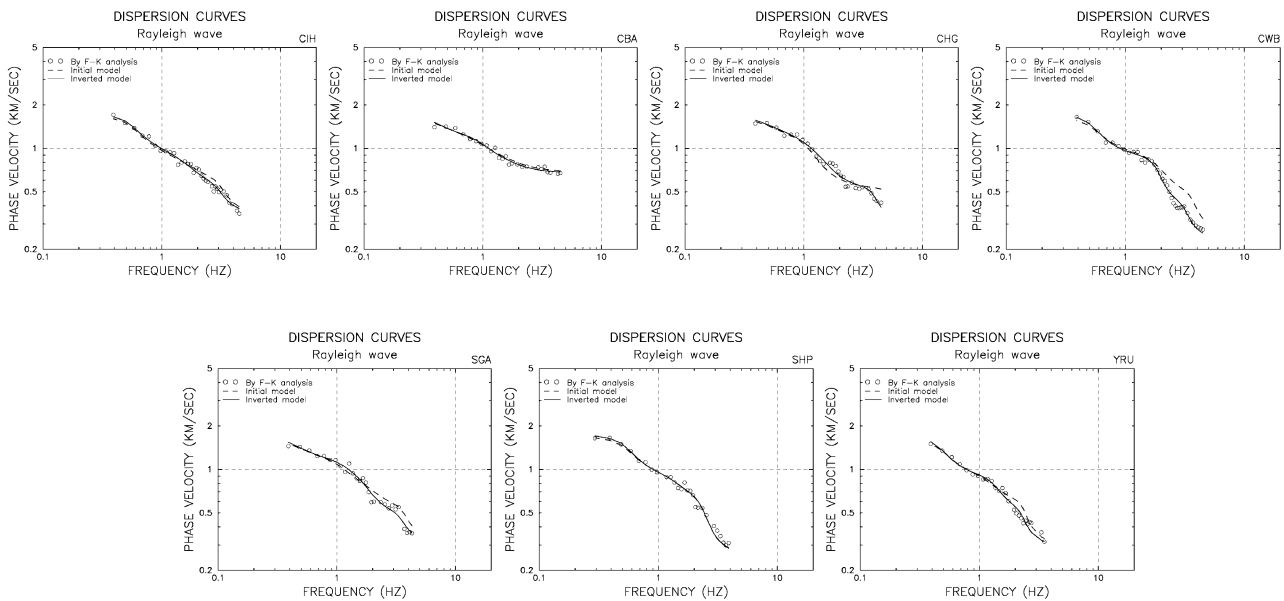


Fig. 12. Observed phase velocities (open circles) and theoretical phase velocities of the fundamental mode of the Rayleigh wave with initial (dashed lines) and inverted structures (solid lines).

the following:

- (1) 50–100 m depths: the northeast part (CBA) of the city has higher velocities;
- (2) 200–300 m depths: the northern part (CWB) of the city has higher velocities;
- (3) 400–900 m depths: the eastern part (CHG) of the city has higher velocities;

(4) 1,000–1,100 m depths: the central part (CIH) of the city has higher velocities;

(5) The western part (YRU) of Chia-Yi City has a lower velocity at all depths from 50 to 1,100 m.

On the basis of the gradient changes in velocity structure derived from the differential inversion (Fig. 9), we are able to regroup the layered structure. Therefore, the in-

verted structure can be simplified to be an eight-layer structure. Based on these simplified velocity models, we use the stochastic inversion technique (Herrmann, 1991) to invert the *S*-wave velocity structures at the seven sites; the results are shown in Fig. 11. Based on the inverted structure, we can calculate the theoretical phase velocities of the fundamental mode of the Rayleigh wave. The theoretical phase velocity (the solid lines) closely resembles the observed phase velocities (the open circles), as shown in Fig. 12. This indicates that the inverted velocity structures are reasonable. Based on Fig. 11, we can roughly divide the shallow velocity structure (0–1,500 m) into five layers (the 1st layer: $V_S < 400$ m/s; the 2nd layer: $400 \leq V_S < 700$ m/s; the 3rd layer: $700 \leq V_S < 1,200$ m/s; the 4th layer: $1,200 \leq V_S < 1,500$ m/s; the 5th layer: $V_S \geq 1,500$ m/s), and these results are tabulated in Table 2. In order to examine the spatial variations in the velocity structures, we discuss the changes of the *S*-wave velocities along two cross-sections a-a' and b-b' (Fig. 1). The results can be depicted as:

(a) a-a' (YRU-SHP-CIH-CHG): Line a-a' is a horizontal cross-section across the western and the eastern areas of the city. Layers 1–3 at CHG are the thinnest, while those at YRU are the thickest. The depth of the alluvium gradually increases from the east (CHG) to the west (YRU).

(b) b-b' (CWB-SHP-SGA): Line b-b' is a vertical cross-section across the western section of the city. The depth of the alluvium gradually increases from the north (CWB) to the south (SGA).

5. Conclusions

The objective of this study was to estimate *S*-wave velocity structures in an area of Chia-Yi, Taiwan. To achieve this, we performed microtremor array measurements for a total of 28 arrays deployments at seven sites in Chia-Yi City. According to the *f*-*k* analysis for those frequencies lower than about 1 Hz, propagation directions are concentrated in the northwest and southwest quadrants. This result indicates that the source of the microtremor in this frequency range come from the Taiwan Strait. The derived dispersion curves show that the harder site (CBA) has higher phase velocities than the softer sites (CWB, SHP and YRU), which have lower phase velocities, especially at frequencies between 1 and 5 Hz.

According to the results on inversion, the alluvial layer in Chia-Yi City is about 1,000–1,200 m thick if the *S*-wave velocity of the bedrock is assumed to be 1,500 m/s. The shallow velocity structures (0–1,500 m) can be roughly divided into approximately four to five layers. The depth of the alluvium gradually increases from the east to the west and from the north to the south.

Acknowledgments. The authors would like to express their gratitude to Drs. R. D. Hwang and W. G. Huang for providing the programs and for their stimulating discussions. The authors also appreciate the efforts of the Engineering Seismology Laboratory of NCCU, which provided the microtremor measurements in the field. They also wish to thank Drs. T. Satoh, H. Yamanaka and H. C. Chiu for their valuable comments and suggestions on this article. The National Science Council, Taiwan has supported this research (NSC 92-2119-M-194-004).

References

- Capon, J., High-resolution frequency-wavenumber spectral analysis, *Proc. IEEE.*, **57**, 1408–1419, 1969.
- Chung, J. K. and Y. T. Yeh, Shallow crustal structure from short-period Rayleigh wave dispersion data in southwestern Taiwan, *Bull. Seismol. Soc. Am.*, **87**, 370–382, 1997.
- Herrmann, R. B., Surface wave inversion program (from computer program in Seismology volume IV), 1991.
- Ho, C. S., *An Introduction to the Geology of Taiwan*, Central Geology Survey, the Ministry of Economic Affairs, Taiwan, 1986.
- Horike, M., Inversion of phase velocity of long-period microtremors to the *S*-wave velocity structure down to the basement in urbanized area, *J. Phys. Earth*, **33**, 59–96, 1985.
- Huang, H. C., Characteristics of earthquake ground motion and H/V of microtremor in the southwestern part of Taiwan, *Earthquake Eng. Struct. Dyn.*, **31**, 1815–1829, 2002.
- Huang, W. G. and Y. T. Yeh, The characteristics of microtremors at the site of SMART1 array, *TAO*, **1**, 225–242, 1990.
- Hwang, R. D. and G. K. Yu, Shear-wave velocity structure of upper mantle under Taiwan from the array analysis of surface waves, *Geophys. Res. Lett.*, **32**, L07310, 2005.
- Hwang, R. D., G. K. Yu, W. Y. Chang, and J. P. Chang, Lateral variations shallow shear-wave structure in southern Taiwan inferred from short-period Rayleigh waves, *Earth Planets Space*, **55**, 349–354, 2003.
- Jackson, D. D., Interpretation of inaccurate, insufficient, and inconsistent data, *Geophys. J. R. Astron. Soc.*, **28**, 97–109, 1972.
- Kawase, H., T. Satoh, T. Iwata, and K. Irikura, *S*-wave velocity structures in the San Fernando and Santa Monica area, Proc. of the 2nd International Symposium on Effect of Surface Geology on Seismic Motions, Tokyo, Japan, Vol. 2, 733–740, 1998.
- Kramer, S. L., *Geotechnical Earthquake Engineering*, Prentice-Hall, Upper Saddle River, New Jersey, 1996.
- Kudo, K., T. Kanno, H. Okada, O. Ozel, M. Erdik, T. Sasatani, S. Higashi, M. Takahashi, and K. Yoshida, Site-specific issues for strong ground motions during the Kocaeli, Turkey, earthquake of 17 August 1999, as inferred from array observations of microtremors and aftershocks, *Bull. Seismol. Soc. Am.*, **92**, 448–465, 2002.
- Lacoss, R. T., E. J. Kelly, and M. N., Tokoz, Estimation of seismic noise structure using array, *Geophysics*, **29**, 21–38, 1969.
- Liu, H. P., D. M. Boore, W. B. Joyner, D. H. Oppenheimer, R. E. Warrick, W. Zhang, J. C. Hamilton, and L. T. Brown, Comparison of phase velocities from array measurement of Rayleigh waves associated with microtremor and results calculated from shear-wave velocity profiles, *Bull. Seismol. Soc. Am.*, **90**, 666–678, 2000.
- Mack, R. and E. A. Filtn, Analysis of the spatial coherence of short-period acoustic-gravity waves in the atmosphere, *Geophys. J. R. Astron. Soc.*, **26**, 255–269, 1971.
- Matsushima, T. and H. Okada, Determination of deep geological structures under urban areas using long-period microtremors, *Butsuri-Tansa*, **43**, 21–33, 1990.
- Menke, W., *Geophysical Data Analysis: Discrete Inversion Theory*, Elsevier, New York, 1984.
- Satoh, T., H. Kawase, and S. Matsushima, Estimation of *S*-wave velocity structures in and around the Sendai basin, Japan, using array records of microtremors, *Bull. Seismol. Soc. Am.*, **91**, 206–218, 2001a.
- Satoh, T., H. Kawase, T. Iwata, S. Higashi, T. Sato, K. Irikura, and H. C. Huang, *S*-wave velocity structure of the Taichung basin, Taiwan, estimated from array and single-station records of microtremors, *Bull. Seismol. Soc. Am.*, **91**, 1267–1282, 2001b.
- Shih, R. C., The shallow velocity structure study in the Chia-Nan area (III), NSC Tech. Rep., Taiwan, 1995 (in Chinese).
- Shih, R. C. and Z. G. Fang, The shallow velocity structure study in the Chia-Nan area (II), NSC Tech. Rep. Taiwan, 1994 (in Chinese).
- Shih, R. C., Z. X. Hu, and R. J. Huang, The shallow velocity structure study in the Chia-Nan area (I), NSC Tech. Rep., Taiwan, 1993 (in Chinese).
- Wiggins, R. A., The general linear inverse problem: implication of surface waves and free oscillations for earth structure, *Rev. Geophys. Space Phys.*, **10**, 251–281, 1972.
- Woods, J. W. and P. R. Lintz, Plane waves at small array, *Geophysics*, **38**, 1023–1041, 1973.